Tautomer Interconversion of 2,4-Pentanedione During Gas Chromatography on an Oxidized Cyano-Modified Capillary Column

P.J. Skrdla*, V. Antonucci, and **C. Lindemann**
Merck & Co., Inc., P.O. Box 2000, Rahway, NJ 07065-0900

Abstract

The tautomerization of 2,4-pentanedione (acetylacetone) is examined on a microbore column containing an acid-modified stationary phase made by oxidizing a commercially available cyano-modified column. This stationary phase is found to provide separation of the two tautomers, which allows the kinetic and thermodynamic properties of the on-column interconversion to be investigated. The enol-to-keto tautomerization is found to occur primarily in the stationary phase, being enthalpically driven. By treating the column as a reactor, the interconversion is investigated as a function of temperature. Monitoring the loss of the more gas-stable 'enol' tautomer makes it possible to extract an energy of activation for the net tautomerization (42.7 kJ/mol), because the reaction is found to obey pseudo first-order kinetics. Simple peak-shape analysis of the major component (enol), which is used commonly in treatments of peak tailing, provides insight into the nature of the retention processes of the two tautomers as well as information on chromatographic optimization.

Introduction

Interest in dynamic processes occurring in chromatographic systems dates back to the late 1950s (1). Since then, so-called 'column reactors' have been used to model first-order reversible reactions (2) as well as second-order kinetics (3). When performing such modeling, rate constants can be extracted by fitting theoretical peak-shape equations to the experimentally obtained chromatograms. One application of the first-order column reactor model is the study of dynamic 'enantiomerization' processes (4). A second important application deals with investigations of the origins of peak splitting and tailing, as pertaining to the interconversion of analyte molecules (5). Similarly, retention processes have been investigated using studies of on-column reaction kinetics (6). The study of an on-column tautomerization, as discussed in this work, allows not only the characterization of certain kinetic and thermodynamic properties of the interconversion, but also offers insight into the nature of the retention behavior of the two tautomers.

Many types of molecules have been observed to interconvert during chromatographic analysis. Some of the systems that have recently been studied include the enantiomerization of *N*-benzyl-1,3,2-benzodithiazole-1-oxide (7), the conformer interconversion of Tritostin A (and its under-*N*-methylated synthetic analogue) (8), and the interconversion of 3-amino-2-cyanoacrylate (9). In addition, the thermally activated tautomerization of 2-(2,4-dinitrobenzyl)pyridine has also been studied (10), but not in a chromatographic context. However, most of these studies utilized reversed-phase liquid chromatography. In the gas phase, the interconversion of polychlorinated biphenyls on a modified cyclodextrin stationary phase (11) and the enantiomerization of diaziridines on chiral inclusion stationary phases (12) have been investigated, but the kinetic and thermodynamic characterization of a predominantly surface-driven on-column tautomerization (such as that observed in this study for 2,4-pentanedione) has not been reported to our knowledge. Unlike most studies of 'dynamic enantiomerization' phenomena in which the enantiomers are injected onto the column in a 1:1 ratio, in this work the analyte sample (existing predominantly as a single tautomer species in the gas phase) was injected onto the column and the equilibrium-driven interconversion to the second tautomer investigated.

A different class of column reactors use the stationary phase solely as a catalytic support for the conversion of reactant (substrate) molecules to products (no on-column dynamic processes are monitored). For example, a liquid chromatographic (LC) reactor for the oxidation of phenols (13) has been reported. Similarly, immobilized enzymes have been implemented in packed column continuous-flow systems (14). Because these systems rely solely on surface reactions, the potential role of the stationary phase in dynamic (reversible) on-column processes can also be inferred.

Investigations into the role of surface chemical interactions in dynamic on-column processes closely parallels studies of reten-

* Author to whom correspondence should be addressed: email peter_skrdla@merck.com.

tion mechanisms (6), which are known to be responsible for chromatographic peak tailing and splitting. Most of the work addressing issues surrounding peak tailing in linear (15) and nonlinear (16) chromatographies has dealt with LC systems, and has not yet been extended to dynamic processes. Nevertheless, the modeling of peak tailing in these more simple systems has led to an understanding that a mixed retention mechanism can often be responsible for a wide range of atypical peak shapes. The heterogeneous mass-transfer kinetics of a relatively small fraction of surface adsorption sites with a high interaction strength and slow adsorption/desorption kinetics often contribute to only moderate changes in retention behavior, but they can dramatically affect peak shape. In addition, under some conditions, severe peak tailing can be observed while a relatively high column efficiency is maintained (15). Wirth et al. (17,18) with the aid of fluorescence spectroscopy have observed that only a very small number of active surface sites are necessary for peak asymmetry to become very pronounced.

In this work, the on-column reversible tautomeric behavior of 2,4-pentanedione was investigated by gas chromatography (GC). With the aid of an acid-modified stationary phase, the two tautomeric forms of the compound could be easily distinguished and certain kinetic and thermodynamic parameters pertaining to the interconversion quantitated. The dramatically different retention behavior of the two tautomers facilitated investigations into the nature of the retention mechanisms. With the aid of simple peak-shape analysis (not typically employed for cases in which 'reaction chromatograms' are obtained), insight into the nature of the chemical interactions of this surface-active compound was gained, and conclusions about optimal chromatographic conditions were drawn.

Experimental

Materials

2,4-pentanedione (acetylacetone, ≥ 99%) and dichloromethane (99.9%, HPLC grade) were obtained from Aldrich. A solution of 2,4-pentanedione in dichloromethane (approximately 2%, v/v) was used to obtain all of the chromatograms so that the peak areas between chromatograms could be compared directly.

Columns

A 60-m-long Rtx-1701 GC column (Crossbonded, 14% cyanopropylphenyl–86% dimethyl polysiloxane, Restek Corporation) with a 0.32-mm i.d. and 1.0-µm film thickness was used to collect all of the data presented in this study. The column stationary phase was first oxidized by exposure to air (220°C for > 24 h). Rtx-1301 (6% cyanopropylphenyl–94% dimethyl polysiloxane, also oxidized), Rtx-1 (100% dimethyl polysiloxane), and Stabilwax (Crossbond Carbowax, poly(ethylene)glycol) columns were investigated quantitatively in order to allow for comparison of the chromatography.

GC instrumentation

Gas 'reaction chromatograms' were obtained under isothermal and isobaric conditions on a Hewlett-Packard HP6890 GC system equipped with a flame ionization detector (FID), a Hewlett-Packard 5973 mass-selective detector, and dual split/splitless injection ports. The oven temperature was varied from 105°C to 180°C. The column pressure was maintained at 15.0 psi for all runs with flow rates being recorded at each new temperature. A 1-µL injection volume and a 50:1 injector split ratio were used with six syringe flushes in the wash solvent (dichloromethane) and six sample flushes prior to each injection. The injector and detector temperatures were maintained at 250°C. Duplicate injections were made at each oven temperature, and the chromatograms were analyzed using Turbochrom software (PerkinElmer).

Fourier transform-infrared instrumentation

Infrared (IR) spectra of liquid 2,4-pentanedione (neat) were recorded on a Nexus 670 spectrophotometer (Nicolet) equipped with a DTGS detector using NaCl windows to contain the sample. A total of 32 co-added scans (acquired at 4 cm^{-1} resolution) in the 4000 to 600 cm^{-1} range were compiled for each spectrum. A PC running Omnic E.S.P. software (version 5.1) was used to capture the spectra. A dry nitrogen purge was employed during all data acquisition.

Thermogravimetric analyzer–Fourier transform-instrumentation

Gas-phase IR spectra of 2,4-pentanedione were obtained by heating the liquid from approximately 60°C to near boiling (approximately 138°C) at a heating rate of 10°C/min (spectra collected over the entire heating range) using a TA Instruments Thermal Analyst 2000 thermogravimetric analyzer coupled with a Nicolet Magna IR 550 Fourier transform (FT)-IR spectrophotometer. A PC running Omnic (version 5.2) software was used to capture the spectra. All spectra were acquired under an inert nitrogen atmosphere.

Results and Discussion

Tautomerization of 2,4-pentanedione

The molecule 2,4-pentanedione, having a boiling point of 140.4°C (19), produces a single, sharp peak when chromatographed by GC on most stationary phases (Figure 1). These include alkane, phenyl, and cyano-modified supports as well as poly(ethylene)glycol stationary phases. The peak shape is largely independent of temperature. However, on stationary phases containing acid groups, temperature-dependent peak asymmetry was observed (Figure 2). The acid-functionalized column was prepared by oxidizing the surface cyano groups of an Rtx-1701 column (see Experimental section). GC–mass spectrometry was performed on each peak (I and II, Figure 2) as well as the 'plateau' region between the two in order to investigate the possibility of on-column decomposition or degradation of the analyte. It was found that the mass spectra of all components were consistent with the 2,4-pentanedione molecule (*m/z* 100 parent ion, major fragments at *m/z* 85 and 43), suggesting that on-column degradation/decomposition was not responsible for the observed chromatographic peak shapes. A major fragment at *m/z*

72, routinely observed in the mass spectrum of the minor late-eluting peak (II), was not found in the other mass spectra (containing mainly the major component, I). The height ratio of the *m/z* 72 peak to the parent ion peak was found to be essentially independent of column temperature. This fragment, consistent with the loss of CO (likely from a carbonyl group in the molecule), aided the assignment of the 'keto' structure to peak II (see Figure 3).

Acetylacetone, as a liquid at 40°C, is known to exist 64% in the enolic form (20) and 36% in the keto form (Figure 3). The enolic C–O stretch absorbs at 1613 cm^{-1} in the mid-IR region (Figure 4). The interaction between the keto form and a small amount of the enolic form is believed to be responsible for the 'doublet' centering near 1725 cm^{-1} (C=O stretch region) (20). Not shown is the enolic O–H stretch absorption, which appears as a shallow broad band in the region of 3000 to 2700 cm^{-1}. In the gas phase, as in nonpolar solutions (21), the pentanedione was expected to exist predominantly as the enol tautomer, because the formation of intramolecular hydrogen bonds is favored over intermolecular hydrogen bonds in such environments. In the IR spectrum of the liquid phase dione, the carbonyl 'doublet' was replaced by a single peak in the gas phase, supporting the idea of a single predominant tautomer existing in the gas phase. This band, coupled with the strong enolic C–O stretch absorbance in the spectrum, aided in the identification of the major peak in the GC chromatograms as the enol tautomer (I). It should be noted that it is not surprising that the keto tautomer was not observed in the gas-phase IR spectrum of the pentanedione (even at lower temperatures), because from the chromatographic peak areas this tautomer was expected to be present in the gas phase at levels well below the detection capabilities of this spectroscopic technique (especially given the intensity of the interfering spectral pattern of the more abundant enol tautomer).

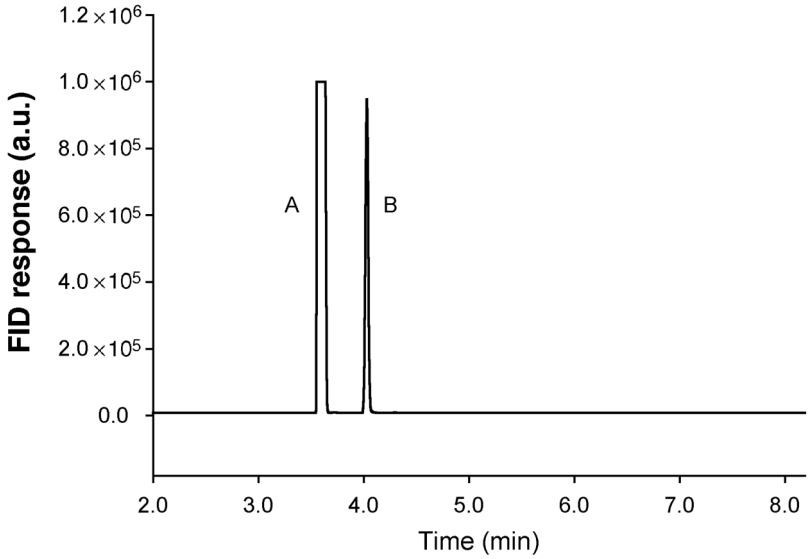

Figure 1. Chromatogram of 2,4-pentanedione (2%, v/v, peak B) in dichloromethane (peak A) obtained on a Rtx-1 column at a column temperature of 135°C.

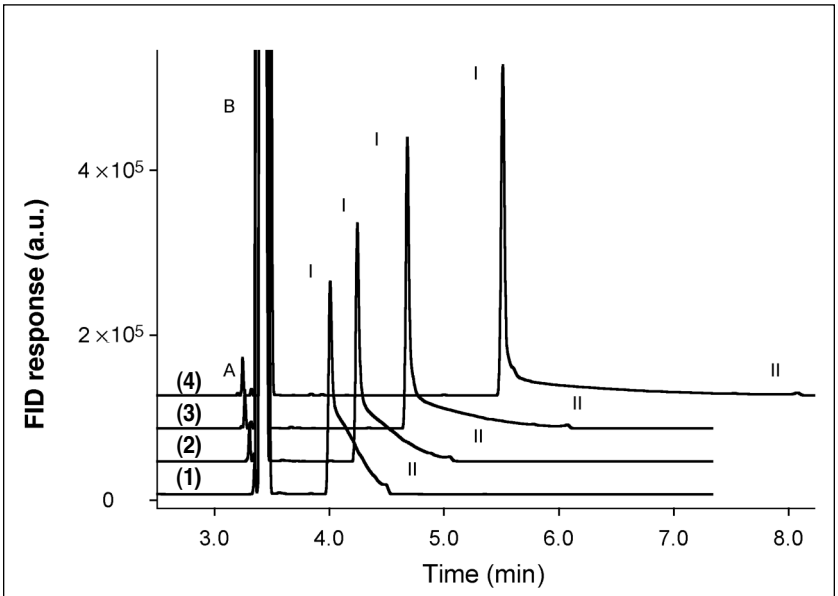

Figure 2. Plot of 'reaction chromatograms' obtained at (1) 180°C, (2) 160°C, (3) 140°C, and (4) 120°C on an oxidized Rtx-1701 column for a solution of 2,4-pentanedione in dichloromethane (approximately 2%, v/v) (peak B). Peak A was used to set the void time. Peaks labeled I and II are a result of the analyte, as described in the text.

The acid-modified stationary phases investigated in this study (oxidized Rtx-1701 and 1301 columns) provided separation of the tautomeric components, which could not be achieved (under similar chromatographic conditions) using the other columns. Although each tautomer exhibited a significantly different strength of interaction with the stationary phase, the general peak shape and elution order was consistent on each of these columns. From Figure 5, it is evident that the keto form has the potential to more strongly interact with the stationary phase through hydrogen bonds than the enol tautomer. This interaction mechanism provides more retention for the keto form and supports the tautomer elution order observed in all of the chromatograms (as will be discussed).

Chromatographic peak shape

Peak shapes similar to the ones reported in this study have been observed in the LC of large cyclosporin molecules, which have both *cis* and *trans* conformations (5). These peak shapes could be explained on the basis of the reaction kinetics of the interconverting isomers. In this work, we present the interconversion of two relatively small tautomers during GC, but are able to invoke a similar quantitative treatment for the peak shape. Each peak in the chromatograms (Figure 6) represents each of the two tautomers whose configuration has remained either 'enol' or 'keto' for the entire time on the column required to achieve the observed peak resolution. Because the tautomerization was sufficiently slow, a

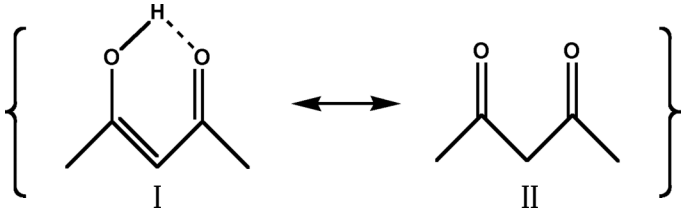

Figure 3. Graphic representation of enol (I, single resonance structure shown intramolecularly hydrogen bonded) to the keto tautomerization of 2,4-pentanedione (II).

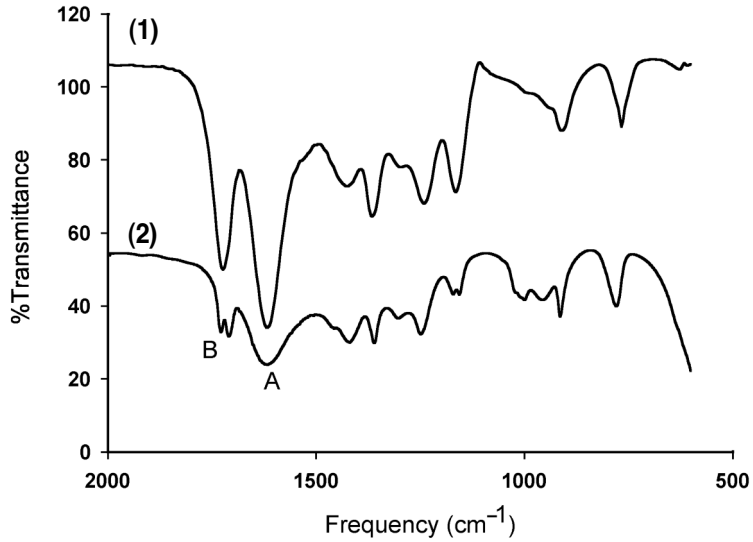

Figure 4. FT-IR spectra (offset vertically from each other by a factor of 40% T) of neat 2,4-pentanedione in (1) the gas collected at 134.5°C and (2) liquid collected at 22°C phases. Peak A arises from the enol tautomer, and the 'doublet' peak (B) originates from the presence of the keto form in the liquid phase.

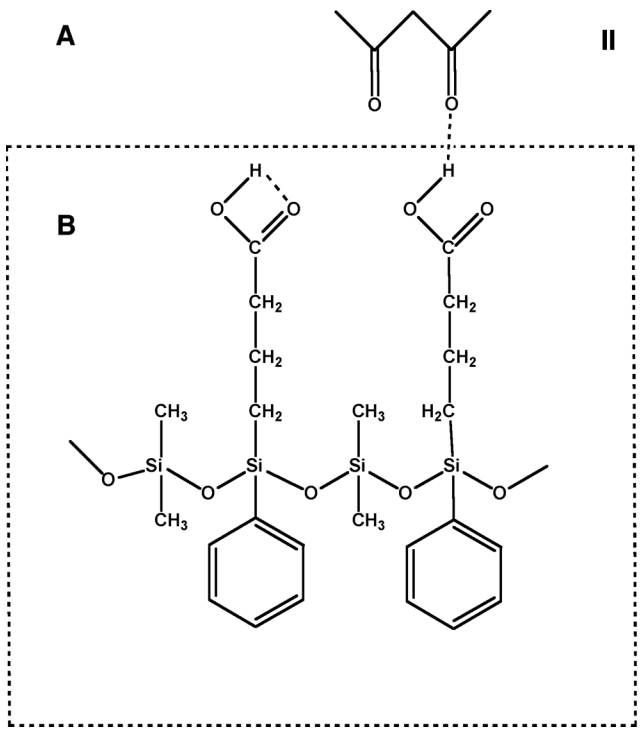

Figure 5. Depiction of the possible mode of interaction of the keto tautomer (II) with the acid-modified GC stationary phase (B) via a hydrogen-bonding interaction. The mobile (gas) phase is denoted as A.

'tailing/plateau' region existed between the two peaks, representing the fraction of molecules that had interconverted at least once on the column prior to elution. It should be noted that unlike more 'typical' interconversion phenomena (i.e., 'enantiomerizations') (22) presented in the literature in which both peaks are of similar area (the ratio of enantiomers injected onto the column is usually 1:1), the chromatograms obtained in this study consistently showed a large enol peak, a small keto peak, and often a substantial plateau region between the two. From the spectroscopic data, it is apparent that the gas-phase stability of the enol was far superior to the keto form (the size of the peaks reflecting these relative thermodynamic stabilities). It should be noted that it was not possible to significantly enhance the relative size of the keto peak by performing cold on-column injection, thus implying that the interconversion was affected more by on-column conditions than the initial conditions of injection. The plateau region increased in length (time axis) at the lower column temperatures, but increased in overall area only at higher temperatures. At lower column temperatures, the probability that no interconversion (based on the relative area of the plateau region) of the two tautomers occurs is greater, and because each tautomer migrates down the column at a different rate, two distinct peaks were observed. At higher temperatures, the probability of interconversion increases, thus a larger area plateau region was observed.

In order to quantitatively examine the effect of flow rate on peak shape under isothermal conditions (column temperature of 135°C), the carrier gas flow was lowered from 1.8 mL/min to 0.6 mL/min by increments of 0.4 mL/min. At the low flow rates, both the enol and the keto peaks were found to diminish in size (not shown), because increasing the column residence time allowed most of the molecules sufficient time to undergo interconversion. In so doing, the area of the plateau region was correspondingly enhanced.

The surface acid groups, believed responsible for providing tautomer peak separation (mentioned previously), are further believed to slow the interconversion of the tautomers by tightly binding (especially) the more strongly retained keto form. It was found that the extent of on-column tautomerization was affected by the concentration of surface acid groups based on the observation that significantly more tautomer interconversion was observed on an oxidized Rtx-1301 column (maximum of a 3% surface acid group coverage) than on the Rtx-1701 (approximately 7% coverage) under identical chromatographic conditions. However, it should be noted that more retention (for both species) and peak

separation was obtained on the oxidized Rtx-1701 relative to the oxidized Rtx-1301 column (consistent with the interaction mechanism in Figure 5). The dependence of the extent of tautomerization on the surface density of acid groups will be investigated further in future work.

Kinetic determination of 2,4-pentanedione tautomerization in the stationary phase

The kinetics of the on-column tautomerization of 2,4-pentanedione responsible for the observed peak shapes on the oxidized Rtx-1701 column were investigated. The chromatographic parameters of interest are given in Table I. From the peak areas of the 'untautomerized fractions' of the enol tautomer (I, integrated approximately as depicted by the broken lines in Figure 6) measured as a function of temperature, the activation energy for the interconversion was determined. In order to do this, it was necessary to correlate both of these variables with the time the molecules spent on column (correcting for flow rate differences at the different temperatures). It has already been shown (quantitatively) that at higher temperatures more of the untautomerized enol becomes interconverted, and at lower temperatures the opposite is true. In addition, it was observed that the degree of tautomerization was affected by the column residence time (as well as the concentration of surface acid groups offered by different columns, but this relationship has not yet been established). These factors made it possible to define the kinetics of the tautomerization on the oxidized Rtx-1701 column. It should be noted that similar to on-column enantiomerizations (7,12), in which no enantiomer enrichment is involved in the overall process (because the enantiomer interconverting at a lower rate has a longer residence time in the stationary phase), this on-column tautomerization showed apparently consistent enol–keto ratios as a function of residence time on the column. Therefore, only the 'net tautomerization' (i.e., the formation of 'interconverted material' in the plateau region or the loss of noninterconverted 'starting material') was considered in the treatment that will be discussed.

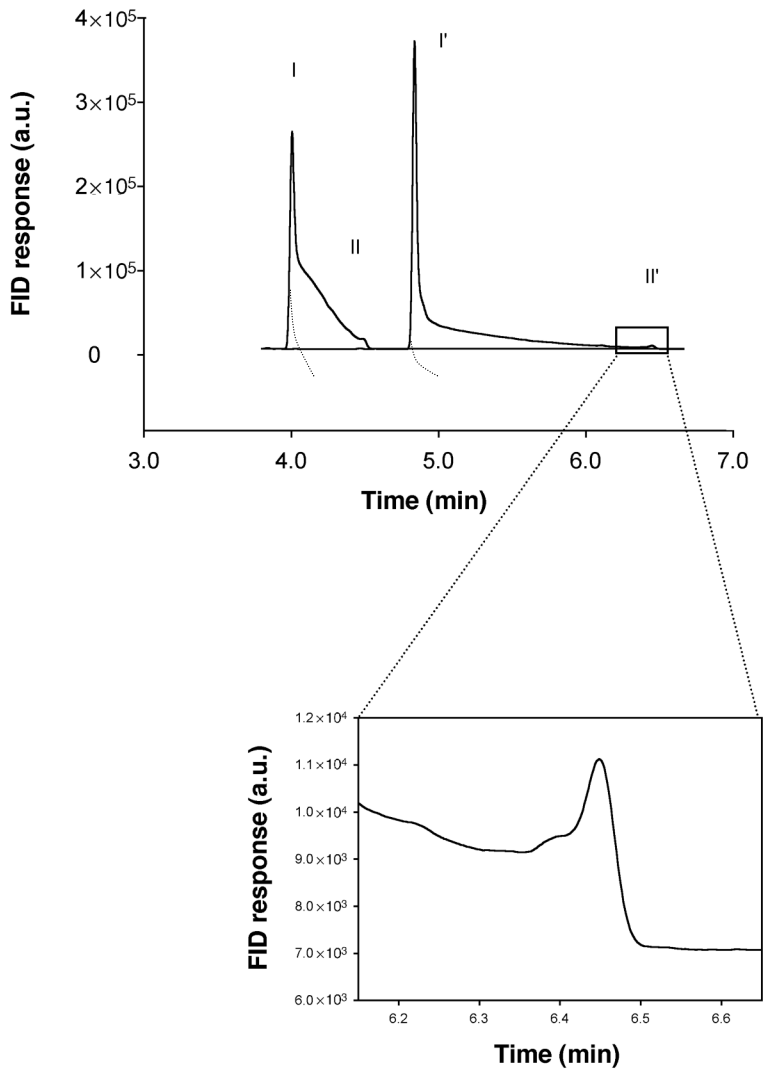

Figure 6. Two overlaid gas chromatograms of 2,4-pentanedione on an oxidized Rtx-1701 GC column obtained at 180°C and 135°C under isobaric conditions. Peaks I and I' represent untautomerized enol material at 180°C and 135°C, respectively, and peaks II and II' represent the keto component at the two different temperatures. The broken lines approximate the area of integration of the enol peak in the two chromatograms. The enlarged chromatogram shows the keto peak in the 135°C chromatogram.

Because the gas phase did not play a significant role in the net on-column tautomerization as a result of the large thermodynamic favorability of the enol form in this phase, only the highlighted (stationary phase) pathway in Figure 7 was considered in the kinetic treatment. The rate of formation of the keto form in the stationary phase is given by:

$$\delta[II]_s/\delta t = \frac{K_s K_{pI}[I]_m}{(1 + K_s)(1 + K_{pI})} \qquad \text{Eq. 1}$$

where $[II]_s$ is the concentration of the keto form in the stationary phase at time t, $[I]_m$ is the concentration of enol tautomer in the gas phase, K_{pI} is the partition coefficient for the enol tautomer partitioning into the stationary phase from the mobile phase, and K_s is the tautomerization equilibrium constant in the stationary phase. $K_s = K_{pII}/K_{pI} = k_{1,s}/k_{-1,s} = k'_{II}/k'_{I}$, according to the principle of microscopic reversibility (12) in which the constants labeled k represent rate constants and k' represents the capacity factors. It should be noted that $k_{1,s} \neq k_{-1,s}$ if tautomer separation occurs, because $K_{pII} \neq K_{pI}$.

Equation 1 is also valid for modeling the net loss of 'untautomerized enol molecules' (e.g., peaks I or I' in Figure 6) as a function of temperature, because the reaction stoichiometry is 1:1. Because equation 1 can be considered constant (defined as k"), the reaction is pseudo first order:

$$\delta[II]_s/\delta t = k'' [I]_m \qquad \text{Eq. 2}$$

Thus treating the column as a reactor, the rate constants at each temperature could theoretically be determined as a function of the residence time in the stationary phase. However, experimentally, this would involve changing the flow rate in order to affect isothermal changes in the retention

times (t_R). Changing the flow rate changes the column pressure, and thus potentially disturbs any equilibrium processes (the dramatic change in the overall peak shape caused by altering the flow rate, described earlier, should be noted). Altering any equilibrium constants could affect the determination of the rate constants (k"), thus this option was not pursued (all chromatography being performed at constant pressure). Instead, in order to obtain the activation energy barrier for the process, a simple mathematical treatment of the data was employed. It should be noted that the pressure drop down the column can be neglected for first-order reactions (23,24). For a first-order process based on the exponential decay of starting material (i.e., the 'enol' tautomer in the gas phase), using k" as the rate constant:

$$[I]_m = [I]_{0,m} \exp(-k''t) \qquad \text{Eq. 3}$$

where $[I]_{0,m}$ and $[I]_m$ are the 'initial' and 'final' concentrations, respectively, of the untautomerized fraction of enol tautomer remaining in the gas phase after time t spent in the stationary phase. We arbitrarily considered the amount of enol injected onto the column at t = 0 to be 100%. This assumption does not affect the calculation of the activation energy (a ratio of concentrations will be considered). By rearrangement, an expression for the rate constant was obtained:

$$k'' = \frac{-\ln([I]_m/[I]_{0,m})}{t} \qquad \text{Eq. 4}$$

The Arrhenius equation can be written as:

$$E_a = -RT \ln (k''/A) \qquad \text{Eq. 5}$$

where E_a is the activation energy (J/mol), R is the gas constant (8.3144 $J^{-1}K^{-1}mol^{-1}$), T is the temperature (K), and A is a constant pertaining to the rate of collisions that occur between the enol molecules and stationary phase, irrespective of their energy (the product of A and the exponential term in equation 5 gives the rate of 'successful collisions', which results in tautomerization). Substituting equation 4 into 5 gives:

$$E_a = -RT \ln\left(\frac{\ln([I]_{0,m}/[I]_m)}{(A \cdot t)}\right) \qquad \text{Eq. 6}$$

Dividing equation 6 by E_aT yields:

$$1/T = -R/E_a \ln\left(\frac{\ln([I]_{0,m}/[I]_m)}{t}\right) + R/E_a \ln (A) \qquad \text{Eq. 7}$$

Therefore, according to equation 7, a plot of 1/T versus $\ln\{\ln([I]_{0,m}/[I]_m)/t\}$ should be linear with a slope of $-R/E_a$ and a *y*-intercept of $R/E_a \ln(A)$.

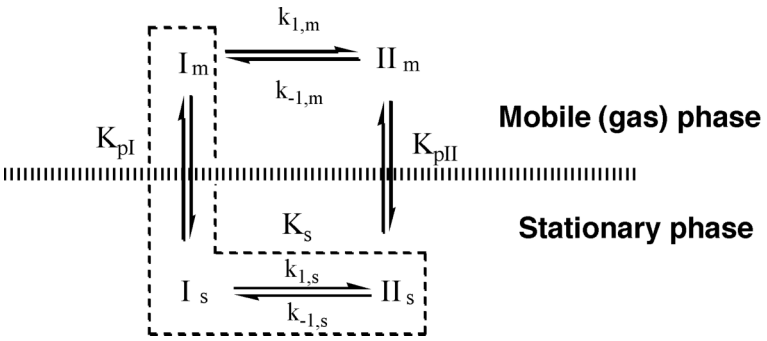

Figure 7. Schematic of all possible pathways for the dynamic, first-order tautomerization of the enol (I) and keto (II) tautomers on a GC column. Only the highlighted (broken-line) pathway was considered for the mathematical treatment of the reaction kinetics.

Table I. Data for the Isobaric, On-Column Tautomerization of 2,4-Pentanedione (Forms I and II) at Various Temperatures on an Oxidized Rtx-1701 column*

%Peak area (I)	Column T (°C)	t_R (I) (min)	t_R (II) (min)	k' (I)	k' (II)	K_s	N (I)
42.03	180	4.006	4.488	0.196	0.340	1.735	3.22×10^2
40.61	175	4.052	4.591	0.214	0.376	1.755	2.93×10^2
38.91	170	4.106	4.718	0.235	0.419	1.785	2.80×10^2
39.13	165	4.168	4.867	0.258	0.469	1.817	2.67×10^2
38.97	160	4.242	5.042	0.284	0.526	1.852	3.09×10^2
38.93	155	4.324	5.240	0.314	0.592	1.887	3.88×10^2
39.54	150	4.423	5.475	0.348	0.669	1.920	6.34×10^2
40.10	145	4.539	5.747	0.388	0.757	1.952	1.97×10^3
40.98	140	4.677	6.071	0.434	0.861	1.985	6.66×10^3
42.85	135	4.837	6.449	0.486	0.981	2.019	1.34×10^4
43.43	130	5.026	6.898	0.546	1.122	2.055	1.89×10^4
44.67	125	5.247	7.432	0.617	1.290	2.092	2.41×10^4
46.01	120	5.509	8.073	0.699	1.489	2.132	4.26×10^4
47.35	115	5.821	8.844	0.794	1.726	2.173	5.74×10^4
48.73	110	6.188	9.769	0.906	2.008	2.217	9.64×10^4
50.15	105	6.622	10.885	1.037	2.348	2.265	1.20×10^5

* The t_R values shown are not corrected for flow rate changes with temperature.

As seen from Figure 8, the linear regression fit of this experimental plot showed a high degree of linearity (R = 0.997, with deviation from linearity only at the higher temperatures in which the error in integrating the 'untautomerized' enol peak becomes more difficult because of peak coalescence). The linearity of this plot confirmed the hypothesis that the net tautomerization is pseudo first order on the oxidized Rtx-1701 column (fixed concentration of surface acid groups). From the graph, the activation energy for the net tautomerization reaction was 42.7 kJ/mol. The value of the pre-exponential term A in the Arrhenius equation was approximately 2.12×10^3 s^{-1}. The magnitude of this activation energy agreed well with the activation energy barrier found for the interconversion of PCB congeners in the gas phase, as reported by Krupcík et al. (11). However, this value also represented approximately half the activation energy reported for the gas-phase enantiomerizations of various other molecules, calculated using the Eyring equation (12,22).

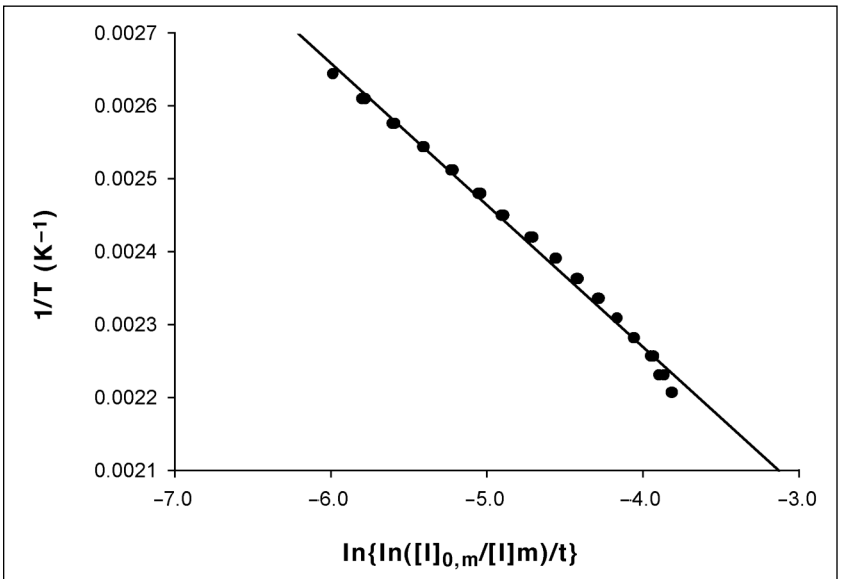

Figure 8. Plot of 1/T versus $\ln\{\ln([I]_{0,m}/[I]_m)/t\}$. The *y*-intercept has a value of (1.491 ± 0.014) × 10^{-3} K^{-1}, and the slope is (–1.95 ± 0.03) × 10^{-4} K^{-1}.

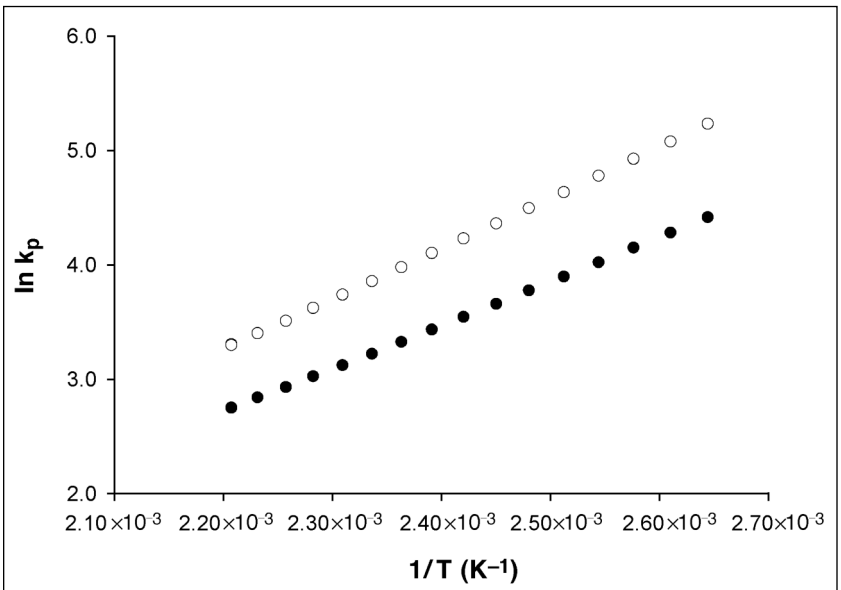

Figure 9. Plots of ln K_p versus 1/T for the enol (I, filled circles) and keto (II, empty circles) forms of 2,4-pentanedione. Each data point represents duplicate measurements (the error in the data was too small to plot). The slopes are 3815 ± 9 K and 4425 ± 7 K for the enol and keto, respectively. The *y*-intercepts are –5.68 ± 0.02 and –6.473 ± 0.016, in the same order. In both cases, the linearity has an R ≥ 0.999.

Thermodynamic analysis of the 2,4-pentanedione on-column tautomerization

Figure 2 demonstrates how not only the peak shape but also the t_R values and peak separation for the keto and enol forms change as a function of temperature. The thermodynamic parameters for the on-column interconversion were obtained through van't Hoff plots of the data contained in Table I. It should be noted that because all t_R values were obtained at constant pressure at the various temperatures, corrections for the changes in flow rate had to be made prior to plotting the data. As mentioned previously, changes in flow rate can affect equilibrium constants through pressure changes, thus all chromatography was performed isobaricly.

Partition coefficients (K_p) for the two tautomers were obtained from the capacity factors (k', where $k' = t_R - t_0/t_0$) shown in Table I, by multiplying them by a factor of 80 (the approximate phase ratio of the mobile phase volume to the stationary phase volume of the column, based on the 1-µm film thickness and 0.32-mm i.d.). The van't Hoff expression, relating the K_p values of each tautomer at each temperature to the enthalpic and entropic changes (ΔH and ΔS, respectively) associated with partitioning into the stationary phase, is given as:

$$\ln K_p = -\Delta H/RT + \Delta S/R \qquad \text{Eq. 8}$$

Figure 9 shows plots of ln K_p versus 1/T for both tautomers of 2,4-pentanedione. From the slopes of the linear regression lines, the change in enthalpy associated with the partitioning/interaction of the enol tautomer with the stationary phase was estimated at –31.72 kJ/mol. For the keto, this value was –36.79 kJ/mol. The greater exothermicity suggests that the partitioning of the enol tautomer into the stationary phase is more favored at higher temperatures. Kinetically, we have observed that more tautomer interconversion also took place at higher temperatures. The entropic terms showed that partitioning into the stationary phase resulted in a loss of entropy for both species. For the enol tautomer, ΔS = –47.2 J/K·mol, and for the keto, ΔS = –53.8 J/K·mol. This data suggests a lower degree of freedom for the keto tautomer on the stationary phase. Because the slopes of the two sets of data points were similar, the predominant retention mechanism for the two species could also be expected to be similar. In both cases, the

strongest interactions likely originated from the acid groups on the surface hydrogen bonding to the pentanedione (as described previously, refer also to Figure 5). The lack of intramolecular hydrogen bonding in the keto tautomer allowed for a much stronger interaction (intermolecular hydrogen bonding) with the stationary phase, thus greater retention, than for the enol form. A plot (not shown) of ln K versus 1/T (refer to Figure 7 and Table I) in which K_s represents the ratio of the capacity factors for the two tautomers yielded a linear plot (R = 0.999) from which a ΔH of –5.07 kJ/mol and ΔS of –6.60 J/K·mol could be extracted. These parameters pertained to the tautomerization occurring in the stationary phase. The values demonstrate that the enol-to-keto transformation in the stationary phase was favorable on this column (from the sign of the Gibbs free energy change for the process) under the conditions investigated. Also, it is evident that the formation of the keto tautomer was driven primarily by enthalpic effects based on the sign and magnitude of this term. This chromatographic result, when coupled with the spectroscopic data in Figure 4, showed that the stationary phase provided a more 'liquid-like' (i.e., polar) environment for the 2,4-pentanedione.

Column efficiency and Stanton numbers

Column efficiency is often used to describe the surface kinetic effects responsible for many commonly observed asymmetrical peak shapes, such as tailing. In this study, we applied a similar treatment to the peak shapes resulting from the interconversion of the 2,4-pentanedione tautomers in an attempt to gain insight into the retention mechanisms. Column efficiency was estimated by measuring the number of theoretical plates (N) for the enol peak using the Foley–Dorsey approximation (25). This approximation used the peak width at 1/10th of the maximum peak height as well as a skewed Gaussian curve to model the peak shape. This model was selected over the 'width-at-half-max approximation', because most of the peaks observed were L-shaped (15) (see Figure 2) and thus column efficiency would not be as accurately represented when the peak tailing is most severe (i.e., at the lower temperatures studied).

Table I shows a correlation of column efficiency with temperature. At the lower temperatures (i.e., as T → 105°C), the efficiency approached 1.2×10^5 theoretical plates; however, as T approached 180°C, N approached 300 plates. This may appear counter-intuitive because the peak 'tailing' increased as the column temperature decreased (as did the separation between the two tautomers). However, even as the tail length increased the enol peak actually appeared to sharpen. This phenomenon was modeled by Fornstedt et al. (15) for a given analyte not interconverting on-column and is generally indicative of slow kinetics of mass transfer at a relatively small number of 'active' surface sites with a high energy of interaction. For analytes in which two forms were interconverting, the peak 'tail' could be explained as the combination of interconversion kinetics and mass-transfer kinetics of two surface-active species at a finite number of active (i.e., acid) sites on the column surface. It should be noted that at the higher temperatures studied, the peak efficiency was lowered because of the incomplete coalescence of both tautomer peaks with the plateau region between them.

Dimensionless Stanton numbers (St) can be used to model peak tailing in analytical (linear) chromatography (26). St is defined as:

$$St = k_f L/\mu \qquad \text{Eq. 9}$$

where k_f is the mass-transfer rate constant (for a particular type of site), L is the column length, and μ is the linear flow rate of the mobile phase. The St number is therefore simply a ratio of the void time to the average residence time of molecules on the surface sites. It can also be expressed as part of an equation in which axial dispersion effects are neglected:

$$N = \frac{(1 + k')^2(St)}{2k'} \qquad \text{Eq. 10}$$

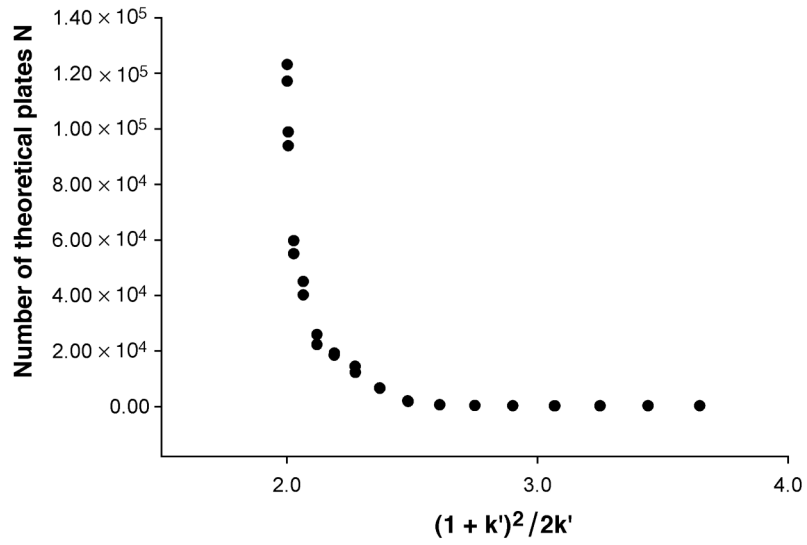

Figure 10. Plot of N for component I versus $(1 + k')^2 / 2k'$ producing a graph with slope equal to St. Data was acquired in duplicate at each temperature.

A plot of N versus $(1 + k')^2/2k'$ is given in Figure 10, the slope of a line joining the data points (not shown) being equal to St. It should be noted that St values are not commonly used to describe peak shapes in dynamic systems. In addition, although it has been suggested that in heterogeneous mass-transfer situations two St values should be used for the purposes of peak-shape modeling (the peak profile being most influenced by the smaller of the two) (26), in this study we considered only the enol peak shape (the major tautomer) and a single St value (the minor component peak being too difficult to integrate accurately). From Figure 10, St can be seen to approach zero as the temperature increases to 180°C, predicting that a split peak should be observed if the interconversion kinetics are neglected (26) (in this case, more of a broad shoulder was observed). As T approached 105°C, St approached infinity, which is usually indicative of a Gaussian and symmetrical peak profile (26).

This is true only if the L-shaped base of the peak is neglected as a result of a combination of interconverting material and stationary phase interactions at 'active' sites. For the temperature region in which $1 < St < 10$, the peak tailed severely and was asymmetrical (26). In general, this data showed that a single St value does not provide much distinction from a classical, noninterconverting system. From a practical standpoint, the plot in Figure 10 suggested that in order to improve the analytical quantitation of the enol tautomer on the oxidized Rtx-1701 column, lower temperatures should be used. In addition, we have observed that higher flow rates should also be employed.

Conclusion

The dynamic GC of 2,4-pentanedione on acid-modified GC stationary phases results in the separation of the keto and enol tautomers, but shows a region of interconversion between the two. The degree of interconversion at a given pressure is dependent on the column temperature, residence time in the stationary phase, and concentration of surface acid groups. The formation of the minor (keto) tautomer is thermodynamically favorable in the stationary phase. However, being less gas-stable, the keto form is likely rapidly converted back to enol upon partitioning out of the stationary phase. It is this behavior that produced the 'plateau/tail' feature observed in the chromatograms. The stationary phase tautomerization from enol to keto was exothermic, with a loss in entropy also accompanying the process. The keto tautomer was more strongly retained on the column, mainly through hydrogen-bonding interactions at the acid sites. The activation energy for the net tautomerization (monitoring the loss of enol 'starting material' injected onto the column as a function of temperature) was estimated at 42.7 kJ/mol, the process obeying pseudo first-order kinetics. Simple peak-shape analysis using theoretical plate calculations and St values showed that the plateau/tail region could be partially explained by mass-transfer kinetics, similar to those responsible for classical tailing in 'nondynamic' chromatography. The peak shape was, however, further complicated by the additional kinetics of the tautomer interconversion.

References

1. J.C. Giddings. Stochastic considerations on chromatographic dispersion. *J. Chem. Phys.* **26:** 169–73 (1957).
2. R. Thede, E. Below, D. Haberland, and S.H. Langer. Theoretical treatment of first-order reversible reactions occurring in a chromatographic reactor, on the basis of consecutive reactions. *Chromatographia* **45:** 149–54 (1997).
3. R. Thede, D. Haberland, Z. Deng, and S.H. Langer. Second-order kinetics in the liquid chromatographic reactor. *J. Chromatogr. A* **683:** 279–91 (1994).
4. R. Thede, D. Haberland, C. Fischer, E. Below, and S.H. Langer. Parametric studies on the determination of enantiomerization rate constants from liquid chromatographic data by empirical peak shape equations for multi-step consecutive reactions. *J. Liq. Chrom. & Rel. Technol.* **21(14):** 2089–2102 (1998).
5. T. Nishikawa, H. Hasumi, S. Suzuki, H. Kubo, and H. Ohtani. Interconversion of cyclosporin molecular form inducing peak broadening, tailing and splitting during reversed-phase liquid chromatography. *Chromatographia* **38(5/6):** 359–64 (1994).
6. B.S. Ludolph, C.-Y. Jeng, A.H.T. Chu, and S.H. Langer. Quantitative study of retention processes in reversed-phase liquid chromatography by means of reaction kinetics. *J. Chromatogr. A* **660:** 3–15 (1994).
7. J. Oxelbark and S. Allenmark. Enantiomerization kinetics studied by dynamic enantioselective liquid chromatography: solvent, temperature and stationary phase effects on the rate of *N*-benzyl-1,3,2-benzodithiazole 1-oxide enatiomer interconversion. *J. Chem. Soc. Perkin Trans.* **8:** 1587–89 (1999).
8. T.V. Alfredson, P.W. Bruins, A.H. Maki, and J.-L. Excoffier. Conformer interconversion in the LC analysis of tritostin A and its under-*N*-methylated synthetic analogue. *J. Chromatogr. Sci.* **32(4):** 132–138 (1994).
9. G. Körtvélyessy, J. Körtvélyessy, T. Mester, G. Meszlényi, and G. Janzsó. Separation and interconversion of 3-amino-2-cyanoacrylates by high-performance liquid chromatography. *J. Chromatogr.* **507:** 409–15 (1990).
10. S. Khatib, S. Tal, O. Godsi, U. Peskin, and Y. Eichen. Site selective processes: a combined theoretical and experimental investigation of thermally activated tautomerization processes in 2(2,4-dinitrobenzyl)pyridine derivatives. *Tetrahedron* **56(36):** 6753–71 (2000).
11. J. Krupcík, M. Májeková, P. Májek, J. Hrouzek, E. Benicka, F. Onuska, P. Sandra, and J. de Zeeuw. On the interconversion energy barriers obtained for atropisomers of some polychlorinated biphenyls by AM1 semiempirical quantum chemistry method and gas chromatography on a modified cyclodextrin stationary phase. *Fresnius J. Anal. Chem.* **352(7/8):** 696–98 (1995).
12. M. Jung and V. Schurig. Determination of enantiomerization barriers by computer simulation of interconversion profiles: enantiomerization of diaziridines during chiral inclusion gas chromatography. *J. Am. Chem. Soc.* **114(2):** 529–34 (1992).
13. Z. Deng, G.R. Dieckmann, and S.H. Langer. Oxidation studies of phenols with cobalt(II) ion-modified silica in a liquid chromatographic reactor. *J. Chem. Soc., Perkin Trans.* **2:** 1123–28 (1998).
14. P. Richter, B.L. Ruiz, M. Sánchez-Cabezudo, and H.A. Mottola. Immobilized enzyme reactors. Diffusion/convection, kinetics, and a comparison of packed-column and rotating bioreactors for use in continuous flow systems. *Anal. Chem.* **68(10):** 1701–1705 (1996).
15. T. Fornstedt, G. Zhong, and G. Guiochon. Peak tailing and mass transfer kinetics in linear chromatography. *J. Chromatogr. A* **741(1):** 1–12 (1996).
16. T. Fornstedt, G. Zhong, and G. Guiochon. Peak tailing and mass transfer kinetics in nonlinear chromatography. *J. Chromatogr. A* **742(1/2):** 55–68 (1996).
17. M. Wirth, M. Ludes, and D. Swinton. Spectroscopic observation of adsorption to active silanols. *Anal. Chem.* **71(18):** 3911–17 (1999).
18. M. Wirth and D. Swinton. Single-molecule probing of mixed-mode adsorption at a chromatographic interface. *Anal. Chem.* **70(24):** 5264–71 (1998).
19. *Aldrich Catalog Handbook of Fine Chemicals, 1998–1999.* 1998, p 1278.
20. R.M. Silverstein, G.C. Bassler, and T.C. Morrill. *Spectrometric Identification of Organic Compounds,* 5th ed. John Wiley & Sons, Inc., New York, NY, 1991, p 115.
21. M. Moriyasu, A. Kato, and Y. Hashimoto. Kinetic studies of fast equilibrium by means of high-performance liquid chromatography. *J. Chromatogr.* **411:** 466–71 (1987).
22. W. Bürkle, H. Karfunkel, and V. Schurig. Dynamic phenomena during enantiomer resolution by complexation gas chromatography. *J. Chromatogr.* **288:** 1–14 (1984).
23. S.H. Langer, J.Y. Yurchak, and J.E. Patton. The gas chromatographic column as a chemical reactor. *J.E. Patton, Ind. Eng. Chem.* **61(4):** 11–21 (1969).
24. S.H. Langer and J.E. Patton. Chemical reactor applications of the gas

chromatographic column. *Advanced Anal. Chem. Instrum.* **11:** 293–73 (1973).
25. J.P. Foley and J.G. Dorsey. Equations for calculation of chromatographic figures of merit for ideal and skewed peaks. *Anal. Chem.* **55:** 730–37 (1983).
26. G. Gotmar, T. Fornstedt, and G. Guiochon. Peak tailing and mass transfer kinetics in linear chromatography. Dependence on the column length and the linear velocity of the mobile phase. *J. Chromatogr. A* **831:** 17–35 (1999).

Manuscript accepted July 17, 2001